

Re-entrant spin glass behavior in Mn-rich YMnO₃

W. R. Chen, F. C. Zhang, J. Miao, B. Xu, X. L. Dong, L. X. Cao, X. G. Qiu, and B. R. Zhao^{a)}
 Laboratory for Superconductivity, Institute of Physics and Center for Condensed Matter Physics,
 Chinese Academy of Sciences, P.O. Box 603, Beijing 100080, China

Pengcheng Dai

Department of Physics and Astronomy, The University of Tennessee, Knoxville, Tennessee 37996 and
 Condensed Matter Sciences Division, Oak Ridge National Laboratory, Oak Ridge, Tennessee 37830

(Received 4 January 2005; accepted 8 June 2005; published online 22 July 2005)

We use magnetism and specific heat measurements to investigate the hexagonal Mn-rich YMnO₃. It is found that upon cooling from a high temperature, the compound first orders antiferromagnetically at $T_N \sim 72$ K and then undergoes a re-entrant spin glass (RSG) transition at $T_{SG} \sim 42$ K. This RSG behavior results from the competition between the ferromagnetic interaction and the antiferromagnetic interaction, which is related to the intrinsic geometric magnetic frustration in this system. © 2005 American Institute of Physics. [DOI: 10.1063/1.1991980]

The doped manganite compounds $R_{1-x}A_x\text{MnO}_3$, with R as the rare-earth or yttrium ion and A as an alkaline-earth ion, have recently attracted considerable attention.^{1,2} It is known that for large and small rare-earth ions, RMnO_3 crystallizes into orthorhombic and hexagonal structures, respectively. For materials with orthorhombic structure, the ground state of undoped RMnO_3 is of long-range antiferromagnetic (AFM) order. When doped, the compound has a rich phase diagram resulting from the interplay among spin, charge, and orbital degrees of freedom. In the case of concentration of A in the regime $0.22 < x < 0.5$, it becomes ferromagnetic (FM) through the double-exchange process.³ On the other hand, one can also make materials that have spin glass (SG) as the low temperature ground state due to the competition between the FM double-exchange interaction and the AFM superexchange interaction.⁴⁻⁶

The hexagonal manganites, such as YMnO_3 , have attracted much attention because of the coupling between ferroelectric and AFM ordering,⁷ but they have not been well studied with regard to doping. Hexagonal YMnO_3 has an A-type AFM structure. The spins of Mn ions within the Mn-O plane form a triangular network and two neighboring Mn ions share the other Mn ion as their nearest neighbor. Since it is impossible to satisfy all nearest-neighbor AFM coupling, the system forms a geometrically frustrated magnetic state. In order to modify the AFM interaction, one may easily think of the traditional method to replace the Y^{3+} partially by cations such as Ca^{2+} or Sr^{2+} . This method was attempted by many researchers but unfortunately turned out to be unsuccessful, for such a little concentration of doped Ca or Sr would bring about an orthorhombic impurity phase in the hexagonal structure.^{8,9} Therefore, a means for modifying the magnetic interaction while maintaining the single hexagonal phase in YMnO_3 is an interesting topic. Substituting Cu in the La site was used to enhance the AFM exchange interaction, hence promoting electronic phase separation in Cu-rich La_2CuO_4 .¹⁰ Off-stoichiometric YMnO_3 composition (Y:Mn ratio 0.95/1 was studied by Lescano *et al.*¹¹ Similarly, the purpose of the present work is to use Mn doping to in-

vestigate the influence of excess Mn on the magnetic properties of the Mn-rich YMnO_3 .

A composition of Y:Mn=1:1.10 (atomic ratio) was selected for studying the effect of excess Mn on magnetic properties since the value of excess Mn, 0.10, is large enough to show the influence of excess Mn on magnetic properties and the sample with this much Mn still reveals single hexagonal phase by the step x-ray diffraction analysis. We found that upon cooling, the Mn-rich YMnO_3 first orders antiferromagnetically, and then undergoes a transition to a SG phase, known as the re-entrant SG (RSG) state. To the best of our knowledge, this is the first example of the RSG behavior found in the hexagonal manganites.

The polycrystalline sample of Mn-rich YMnO_3 was prepared by the conventional solid-state reaction method. For comparison, undoped YMnO_3 was also prepared using the same method. Mixtures of high-purity Y_2O_3 and MnO_2 powders for the samples with different compositions were calcined twice at at 900 °C for 12 h. The powders were sintered at 1450 °C for several days with intermittent grindings to ensure complete reaction. They were then subsequently pulverized, compressed, and sintered at 1450 °C for 12 h to the required compactness for measurements. Powder x-ray-diffraction results indicate that the samples are pure with a single-hexagonal phase. The dc magnetic susceptibility $\chi_{d.c.}$ and hysteresis $M(H)$ were measured with a superconducting quantum interference device magnetometer. The ac magnetic susceptibility $\chi_{a.c.}$ and specific heat $C(T)$ measurements were carried out with a physical property measurement system.

The dc magnetic susceptibility $\chi_{d.c.}$ measurements of Mn-rich YMnO_3 in an applied magnetic field of 100 Oe were performed under both zero-field-cooled (ZFC) and field-cooled (FC) conditions, respectively. The ZFC and FC magnetic susceptibility curves (Fig. 1) start to separate from each other when the temperature is decreased to about 50 K. The ZFC curve displays a sharp peak at around 42 K, where the irreversibility between ZFC and FC curves becomes obvious. Such a $\chi_{d.c.}$ feature is the hallmark of a SG transition. In contrast to Mn-rich YMnO_3 , there is no difference in the ZFC and FC curves of undoped YMnO_3 , consistent with the earlier report.^{7,12} Thus, Mn doping can bring about the formation of a SG state. By fitting the inverse susceptibility

^{a)} Author to whom correspondence should be addressed; electronic mail: brzhao@aphy.iphy.ac.cn

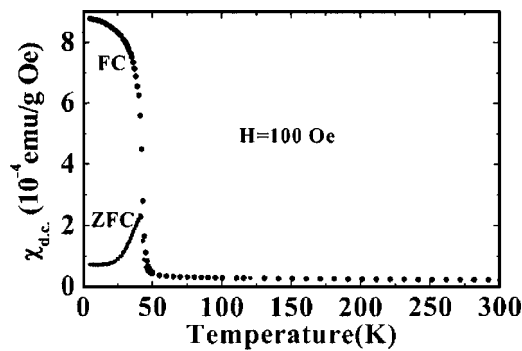


FIG. 1. Temperature dependence of FC and ZFC dc magnetic susceptibility $\chi_{d.c.}$ at $H=100$ Oe for Mn-rich YMnO_3 .

$1/\chi_{d.c.}$ to the Curie–Weiss law $\chi=C/(T-\theta_{CW})$, we obtain the Curie–Weiss temperature $\theta_{CW}=-330$ K for YMnO_3 and $\theta_{CW}=-530$ K for Mn-rich YMnO_3 . Since θ_{CW} is a measure of the AFM coupling strength between Mn ions, the result suggests that the Mn doping enhances the AFM interaction, in contrast to most AFM compounds where impurities usually suppress the AFM interaction. We note that the substitution of Cd for Zn in $\text{Zn}_{1-x}\text{Cd}_x\text{Cr}_2\text{O}_4$ ($x=0.05, 0.10$) also enhances the AFM interaction and drives the system from a frustrated AFM state to a SG ground state in the low-temperature region.¹³ An effective moment of $4.70 \mu_B$ for YMnO_3 and $5.20 \mu_B$ for Mn-rich YMnO_3 are obtained from the Curie constant C , indicating that the excess Mn results in a mixed valence state of Mn^{2+} and Mn^{3+} . This is also confirmed by our x-ray photoelectron spectroscopy measurement. Our present results, the Curie–Weiss temperature, and the effective Mn moment for YMnO_3 , are also relatively consistent with those reported by Tomuta *et al.*¹⁴ and Muñoz *et al.*¹⁵

To further characterize the SG behavior of Mn-rich YMnO_3 , we performed frequency dependent susceptibility measurements. Figure 2 shows the in-phase component of the ac susceptibility as a function of temperature, $\chi_{a.c.}$ versus T . It shows a frequency dependent peak at the temperature where the ZFC dc magnetic susceptibility reaches its maximum. The peak position of $\chi_{a.c.}$ versus T curve (corresponding to the spin freezing temperature T_f) shifts to a higher temperature with increasing frequency and its magnitude depends strongly on the frequency just below T_f . These are also distinct hallmarks of a SG transition.

Figure 3 shows the magnetization of Mn-rich YMnO_3 as a function of magnetic field, $M(H)$, under ZFC at various

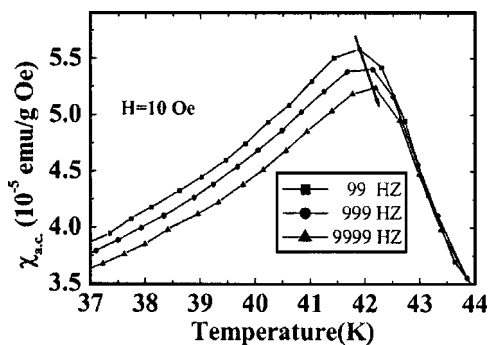


FIG. 2. Temperature dependence of ac magnetic susceptibility $\chi_{a.c.}$ at a frequency of 99, 999, 9999 Hz in an applied field of 10 Oe for Mn-rich YMnO_3 .

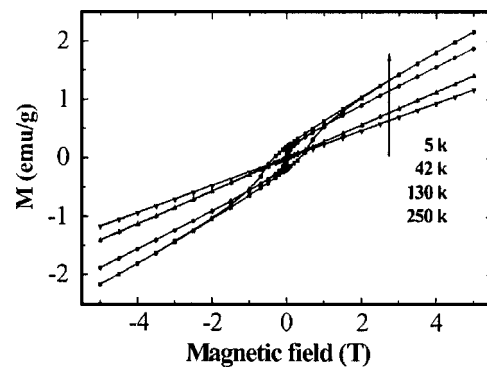


FIG. 3. Typical magnetic-field dependence of the magnetization $M(H)$ under the ZFC conditions at different fixed temperatures for Mn-rich YMnO_3 .

temperatures. At the higher temperatures, the magnetization curves show the paramagnetic (PM) feature. With decreasing temperature, the M versus H curve deviates from the linear relation and bends more, but the magnetization does not show saturation in fields up to 5 T. In addition, the $M(H)$ curve displays an obvious hysteresis at 5 K, consistent with a conventional SG system.^{6,16} Such a result is an indication of weak ferromagnetism below T_f , which may form because of the double-exchange interaction between Mn^{2+} and Mn^{3+} . Such double-exchange interaction between d^4 and d^5 in the Mn^{2+} – Mn^{3+} mixed valance state has been proposed in the Zr-doped $\text{Y}_{1-x}\text{Zr}_x\text{MnO}_3$.^{17,18} We also found that the coercive field H_C increases with decreasing temperature in the SG state to 2.5 kOe at 5 K. It is well known that in a conventional ferromagnet the coercive field is attributable to the blocking of the domain-wall motion. Here, the large values of H_C may be related to the intrinsic geometric magnetic frustration in this system.

The magnetic specific heat for YMnO_3 and Mn-rich YMnO_3 was estimated by subtracting the lattice contribution (which was estimated using the Debye model) from the total measured specific heat. The lattice contribution to the specific heat might be a little overestimated, and therefore a smooth extrapolation of the high-temperature part of the dependence of C_m/T to higher temperature (above 120 K) will come to negative magnetic heat values (Fig. 4). However, this fact does not significantly influence the general conclusions. Sharp lambda-like anomalies are observed at Néel temperatures of $T_N \sim 66$ K for YMnO_3 and $T_N \sim 72$ K for Mn– YMnO_3 demonstrating the AFM transitions. This result confirms the enhancement of AFM coupling in the Mn-rich sample, but we should note that the AFM transition was not obvious in the $\chi_{d.c.} \sim T$ measurement. For YMnO_3 , the dependence of C_m/T on temperature deviates from the $C_m \propto T^3$ law, as is expected in frames of the spin waves model for antiferromagnets below the Néel temperature. This results from the geometric magnetic frustration in this hexagonal system. For Mn-rich YMnO_3 , another anomaly appears at about 42 K, and below that temperature C_m/T decreases linearly with temperature, i.e., $C_m \propto T^2$, similar to geometrically frustrated SG systems, such as the kagomé lattice^{19,20} and the spinel lattice,²¹ and unlike the T-independent behavior of C_m/T found in most conventional SG systems.²² Thus, it very likely reveals the importance of the geometric magnetic frustration effect.

It is therefore clear that the Mn-rich YMnO_3 first orders antiferromagnetically at 72 K from a PM phase to an AFM

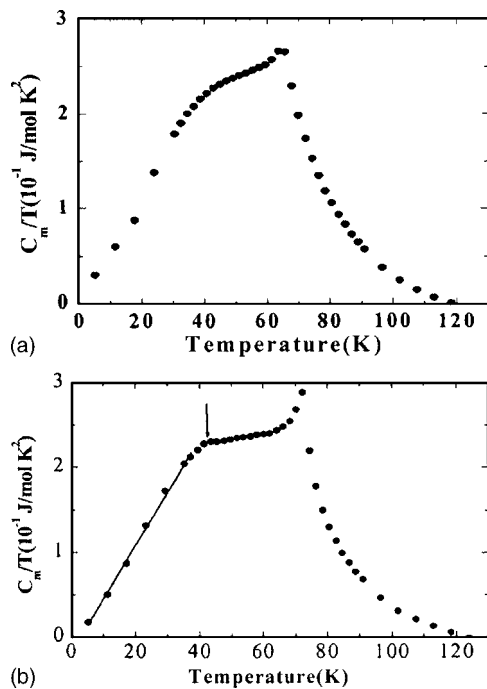


FIG. 4. Magnetic specific heat divided by T for (a) YMnO_3 and (b) Mn-rich YMnO_3 . The Néel temperature and specific heat for YMnO_3 are different from but consistent with previous reports (Refs. 14 and 15).

phase, and then undergoes the transition into a RSG phase below $T_{\text{SG}} \sim 42$ K. We note that the $T_{\text{SG}} \sim 42$ K is comparable to that of the orthorhombic manganite $\text{R}_{1-x}\text{A}_x\text{MnO}_3$ systems such as $(\text{Tb}_{0.33}\text{La}_{0.67})_{0.67}\text{Ca}_{0.33}\text{MnO}_3$ ($T_{\text{SG}} \sim 48$ K) (Ref. 4) and $\text{La}_{0.46}\text{Sr}_{0.54}\text{Mn}_{0.98}\text{Cr}_{0.02}\text{O}_3$ ($T_{\text{SG}} = 40.8$ K).⁶ Moreover, the sample still maintains the hexagonal structure and thus the geometric magnetic frustration in the Mn–O plane. This makes the competition between FM and AFM interactions be related to its intrinsic geometric magnetic frustration, unlike the case of the orthorhombic $\text{R}_{1-x}\text{A}_x\text{MnO}_3$. This striking feature will influence the magnetic properties, such as the dynamic memory effect of the SG state and may lead to some unexpected phenomena.

In summary, we performed the magnetism and specific heat measurements on polycrystalline Mn-rich YMnO_3 . Our data indicate that a RSG phase exists in the present system with a hexagonal structure, and it is ascribed to the competition between the FM and the AFM interaction. This is the first example to show the RSG phenomenon in the hexagonal doped manganites. This newly fabricated Mn-rich YMnO_3

material will enable our in-depth study on the rich physical properties of the doped manganite compounds $\text{R}_{1-x}\text{A}_x\text{MnO}_3$.

This work is supported by the State Key Program for Basic Research of China and the National Natural Science Foundation. One of the authors (P.D.) is supported by the U.S. NSF (DMR-0453804), DOE under Contract No. DE-AC05-00OR22725 with UT-Battelle, LLC, and NSF of China under Contract No. 10128409.

¹R. von Helmolt, J. Wecker, B. Holzapfel, L. Schultz, and K. Samwer, *Phys. Rev. Lett.* **71**, 2331 (1993).

²A. Moreo, S. Yunoki, and E. Dagotto, *Science* **283**, 2034 (1999).

³C. Zener, *Phys. Rev.* **82**, 403 (1951).

⁴J. M. De Teresa, M. R. Ibarra, J. García, J. Blasco, C. Ritter, P. A. Algarabel, C. Marquina, and A. del Moral, *Phys. Rev. Lett.* **76**, 3392 (1996).

⁵T. Terai, T. Kakeshita, T. Fukuda, T. Saburi, N. Takamoto, K. Kindo, and M. Honda, *Phys. Rev. B* **58**, 14908 (1998).

⁶J. Dho, W. S. Kim, and N. H. Hur, *Phys. Rev. Lett.* **89**, 027202 (2002).

⁷Z. J. Huang, Y. Cao, Y. Y. Sun, Y. Y. Xue, and C. W. Chu, *Phys. Rev. B* **56**, 2623 (1997).

⁸B. Fu, W. Huebner, M. F. Trubelja, and V. S. Stubican, *J. Mater. Res.* **9**, 2645 (1994).

⁹D. Vega, G. Polla, A. G. Leyva, P. König, H. Lanza, and A. Esteban, *J. Solid State Chem.* **156**, 458 (2001).

¹⁰X. L. Dong, Z. F. Dong, B. R. Zhao, Z. X. Zhao, X. F. Duan, L.-M. Peng, W. W. Huang, B. Xu, Y. Z. Zhang, S. Q. Guo, L. H. Zhao, and L. Li, *Phys. Rev. Lett.* **80**, 2701 (1998).

¹¹G. Lescano, F. M. Figueiredo, F. M. B. Marques, and J. Schmidt, *J. Eur. Ceram. Soc.* **21**, 2037 (2001).

¹²W. C. Koehler, H. L. Yakel, E. O. Wollan, and J. W. Cable, *Phys. Lett.* **9**, 93 (1964).

¹³H. Martinho, N. O. Moreno, J. A. Sanjurjo, C. Rettori, A. J. García-Adeva, D. L. Huber, S. B. Oseroff, W. Ratchliff II, S.-W. Cheong, P. G. Pagliuso, J. L. Sarrao, and G. B. Martins, *Phys. Rev. B* **64**, 024408 (2001).

¹⁴D. G. Tomuta, S. Ramakrishnan, G. J. Nieuwenhuys, and J. A. Mydosh, *J. Phys.: Condens. Matter* **13**, 4543 (2001).

¹⁵A. Muñoz, J. A. Alonso, M. J. Martínez-Lope, M. T. Casáis, J. L. Martínez, and M. T. Fernández-Díaz, *Phys. Rev. B* **62**, 9498 (2000).

¹⁶I. A. Campbell, S. Senoussi, F. Varret, J. Teillet, and A. Hamzic, *Phys. Rev. Lett.* **50**, 1615 (1983).

¹⁷B. B. Van Aken, Jan-Willem G. Bos, R. A. deGroot, and T. T. M. Palstra, *Phys. Rev. B* **63**, 125127 (2001).

¹⁸T. Katsufuji, M. Masaki, A. Machida, M. Moritomo, K. Kato, E. Nishibori, M. Takata, M. Sakata, K. Ohoyama, K. Kitazawa, and H. Takagil, *Phys. Rev. B* **66**, 134434 (2002).

¹⁹A. P. Ramirez, G. P. Espinosa, and A. S. Cooper, *Phys. Rev. Lett.* **64**, 2070 (1990).

²⁰I. S. Hagemann, Q. Huang, X. P. A. Gao, A. P. Ramirez, and R. J. Cava, *Phys. Rev. Lett.* **86**, 894 (2001).

²¹C. Urano, M. Nohara, S. Kondo, F. Sakai, H. Takagi, T. Shiraki, and T. Okubo, *Phys. Rev. Lett.* **85**, 1052 (2000).

²²L. E. Wenger and P. H. Keesom, *Phys. Rev. B* **13**, 4053 (1976).